学位論文

The mitochondrial calcium uniporter contributes to morphine tolerance through pCREB and CPEB1 in rat spinal cord dorsal horn

（ラット脊髄後角でミトコンドリアカルシウムユニポータは pCREB,CPEB1 を介してモルヒネ耐性に関与する）

旭川医科大学大学院医学系研究科博士課程医学専攻

髙橋　桂哉

（Hyun Yi, Jun Gu, Daigo Ikegami, Shue Liu, Takafumi Iida,
Yuta Kashiwagi, Chuanhui Dong,Takayuki Kunisawa, Shuanglin Hao）

BJA

British Journal of Anaesthesia, 123 (2): e226–e238 (2019)

doi: 10.1016/j.bja.2019.05.027
Advance Access Publication Date: 26 June 2019
Pain Mechanisms and Novel Analgesics

The mitochondrial calcium uniporter contributes to morphine tolerance through pCREB and CPEB1 in rat spinal cord dorsal horn

K. Takahashi[1,2], H. Yi[1], J. Gu[1], D. Ikegami[1], S. Liu[1], T. Iida[1,2], Y. Kashiwagi[1], C. Dong[3], T. Kunisawa[2] and S. Hao[1,*]

[1]Department of Anesthesiology, University of Miami Miller School of Medicine, Miami, FL, USA, [2]Department of Anesthesiology and Critical Care Medicine, Asahikawa Medical University, Asahikawa, Japan and [3]Biostatistics Division, Department of Neurology, University of Miami Miller School of Medicine, Miami, FL, USA

*Corresponding author. E-mail: shao@med.miami.edu

Abstract

Background: The long-term use of opioid analgesics is limited by the development of unwanted side-effects, such as tolerance. The molecular mechanisms of morphine anti-nociceptive tolerance are still unclear. The mitochondrial calcium uniporter (MCU) is involved in painful hyperalgesia, but the role of MCU in morphine tolerance has not been uncharacterised.
Methods: Rats received intrathecal injection of morphine for 7 days to induce morphine tolerance. The mechanical withdrawal threshold was measured using von Frey filaments, and thermal latency using the hotplate test. The effects of an MCU inhibitor, antisense oligodeoxynucleotide against cyclic adenosine monophosphate response element (CRE)-binding protein (CREB) or cytoplasmic polyadenylation element-binding protein 1 (CPEB1) in morphine tolerance were examined.
Results: Spinal morphine tolerance was associated with an increased expression of neuronal MCU, phospho-CREB (pCREB), and CPEB1 in the spinal cord dorsal horn. MCU inhibition increased the mechanical threshold and thermal latency, and reduced the accumulation of mitochondrial calcium in morphine tolerance. Intrathecal antisense oligodeoxynucleotide against CREB or CPEB1 restored the anti-nociceptive effects of morphine compared with mismatch oligodeoxynucleotide in von Frey test and hotplate test. Chromatin immunoprecipitation with quantitative PCR assay showed that CREB knockdown reduced the interaction of pCREB with the *ccdc109a* gene (encoding MCU expression) promoter and decreased the MCU mRNA transcription. RNA immunoprecipitation assay suggested that CPEB1 binds to the MCU mRNA 3′ untranslated region. CPEB1 knockdown decreased the expression of MCU protein.
Conclusions: These findings suggest that spinal MCU is regulated by pCREB and CPEB1 in morphine tolerance, and that inhibition of MCU, pCREB, or CPEB1 may be useful in preventing the development of opioid tolerance.

Keywords: calcium; CPEB; CREB; mitochondrial calcium uniporter; morphine; opioid tolerance; opioids

Editor's key points

- The molecular mechanisms of morphine tolerance are unclear.
- The role of the mitochondrial calcium uniporter (MCU) in morphine tolerance was characterised in a rat model of morphine tolerance induced by intrathecal morphine injection for 1 week.
- Morphine tolerance was associated with increased expression of neuronal MCU, phospho-CREB, and CPEB1 in the spinal cord dorsal horn.
- Inhibition of the MCU and CREB or CPEB1 knockdown increased mechanical threshold and thermal latency, indicating that the spinal MCU is regulated by pCREB and CPEB1 in morphine tolerance.
- Inhibition of the MCU, pCREB, or CPEB1 provide potential novel targets for preventing development of opioid tolerance.

Editorial decision: 07 May 2019; **Accepted**: 7 May 2019

Consumption of prescription opioids has been growing.[1,2] However, long-term opioid use is limited by the development of unwanted side-effects, such as tolerance, hyperalgesia, and dependence/addiction, which contribute to the current epidemic of opioid abuse and overdose-related deaths in the USA.[2–4] Tolerance to opioid analgesia is described as reduced responsiveness to the analgesia produced by opioids. Previous evidence showed that morphine tolerance induces neurotoxicity in spinal neurones[5]; however, the molecular mechanism of morphine tolerance is not clear.

The mitochondrial calcium uniporter (MCU) is a critical protein of the inner mitochondrial membrane mediating Ca^{2+} uptake into the matrix.[6] MCU is involved in the induction of painful hyperalgesia and spinal long-term potentiation (LTP).[7] Chronic morphine induces a facilitated LTP.[8] However, the role of MCU in morphine tolerance is not clear. The transcription factor, cyclic adenosine monophosphate response element (CRE)-binding protein (CREB), has been shown to regulate neural plasticity.[9] Short- and long-term morphine exposure alter phosphorylated CREB (pCREB) expression in different brain regions.[10] Chronic morphine raises pCREB levels in the lumbar dorsal root ganglion and the dorsomedial nucleus of the hypothalamus.[10,11] Repeated morphine exposure causes neuroadaptations in neurones through the activation of CREB.[12] Cytoplasmic polyadenylation element-binding proteins (CPEB) are mRNA-binding proteins associated with protein translation that play an important role in development, health, and disease.[13] Recent evidence shows that CPEB is involved in hyperalgesia priming and pain chronification.[14–16] Of the four CPEB protein subtypes (CPEB1–4),[17] CPEB1 is involved in anxiety and chronic pain.[18] Similar cellular and intracellular changes occur in the spinal cord after peripheral nerve injury and morphine tolerance[19]; however, the role of MCU or CPEB1 in morphine tolerance remains unclear.

pCREB binds at the promoter of the *ccdc109a* gene (encoding MCU expression) and stimulates its expression.[20] However, the relationship of MCU and pCREB or CPEB1 in morphine tolerance is not clear. Here, we report that pCREB mediates the expression of MCU transcription in an epigenetic manner, and that CPEB1 mediates the expression of spinal MCU protein.

Methods

Animals

Before the beginning of the study, male 7–8-week-old Sprague Dawley rats (weight: 210–230 g) obtained from Charles River Laboratories, Wilmington MA USA were housed (one to three per cage) for ~1 week. The rats freely received access to food and water, and were maintained on a 12:12 light:dark schedule at 21°C and 60% humidity. The University of Miami Institutional Animal Care and Use Committee approved the housing conditions and experimental procedures. All procedures were in accordance with relevant aspects of the Animal Research: Reporting of In Vivo Experiments and National Institutes of Health guidelines. An intrathecal catheter was implanted through an incision in the atlanto-occipital membrane, and advanced 8.5 cm caudally to position its tip at the level of the lumbar enlargement, as described[21] (see Supplementary Methods and Results for details).

Anti-nociception testing

We used calibrated von Frey filaments (Stoelting, Wood Dale, IL, USA) to determine the mechanical withdrawal threshold serially to the hind paw in ascending order of strength, as described.[21] Experimenters were blinded to the groups during behavioural tests. Hotplate thermal latency was measured with a hotplate apparatus (IITC Life Science Inc., Woodland Hills, CA, USA). The anti-nociceptive effects of morphine were represented as a percentage of the maximum possible effect (%MPE) using the formula %MPE=([test−baseline]/[cut-off−baseline])×100% (see Supplementary Methods and Results for details).

Quantitative real time polymerase chain reaction

Rat lumbar L4/5 spinal cord dorsal horn (SCDH) tissue was collected and RNeasy Mini Kit (Qiagen, Germantown, MD, USA) was used for total RNA isolation. One microgram of RNA was converted into cDNA, and then real-time polymerase chain reaction (PCR) was performed (see Supplementary Methods and Results for details).

Western immunoblots

Rat SCDH tissue or B35 cells (American Type Culture Collection (ATCC), Manassas, VA) were lysed, homogenised, and sonicated with 1× RIPA protein lysis buffer containing protease and phosphatase inhibitor cocktail (Sigma-Aldrich, St Louis, MO, USA). Proteins were denatured and transferred onto a polyvinylidene difluoride (PVDF) membrane, and the membrane was incubated with primary antibodies overnight at 4°C, including rabbit polyclonal anti-MCU, mouse monoclonal anti-pCREB, goat anti-CPEB1, mouse anti-VDAC1, and mouse monoclonal anti-β-actin. The PVDF membrane was incubated with secondary antibodies, and then developed in chemiluminescence solution (see Supplementary Methods and Results for details).

Chromatin immunoprecipitation with quantitative PCR

For chromatin immunoprecipitation with quantitative PCR (ChIP-qPCR), SCDH tissue was homogenised and fixed with formaldehyde 1% for 10 min, and 2.5 M glycine was used to stop the reaction. Fixed tissue was washed and resuspended with sodium dodecyl sulphate (SDS) lysis buffer 250 µl (50 mM Tris-HCl [pH 8.0], 10 mM ethylenediamine tetra-acetic acid, and SDS 1%), as described[22] (see Supplementary Methods and Results for details).

RNA immunoprecipitation with quantitative PCR

B35 cells were treated with recombinant tumour necrosis factor alpha (rTNFα) (10 ng ml^{-1}) or vehicle,[22] cross linked with formaldehyde 1%, lysed in lysis buffer, and immunoprecipitated with anti-CPEB1 antibody (see Supplementary Methods and Results for details). RNA was extracted and converted into cDNA, and then real-time PCR was performed with Fast SYBR Green Master Mix (Applied Biosystems, Grand Island, NY, USA).

Immunohistochemistry

Immunostaining was carried out, as described.[23] On Day 7 of chronic morphine, 1.5 h after the last morphine dose, the rats were perfused with paraformaldehyde (PFA) 4% in 0.1 M phosphate-buffered saline. The spinal cord was postfixed and cryoprotected. Immunostaining of glial fibrillary acidic protein

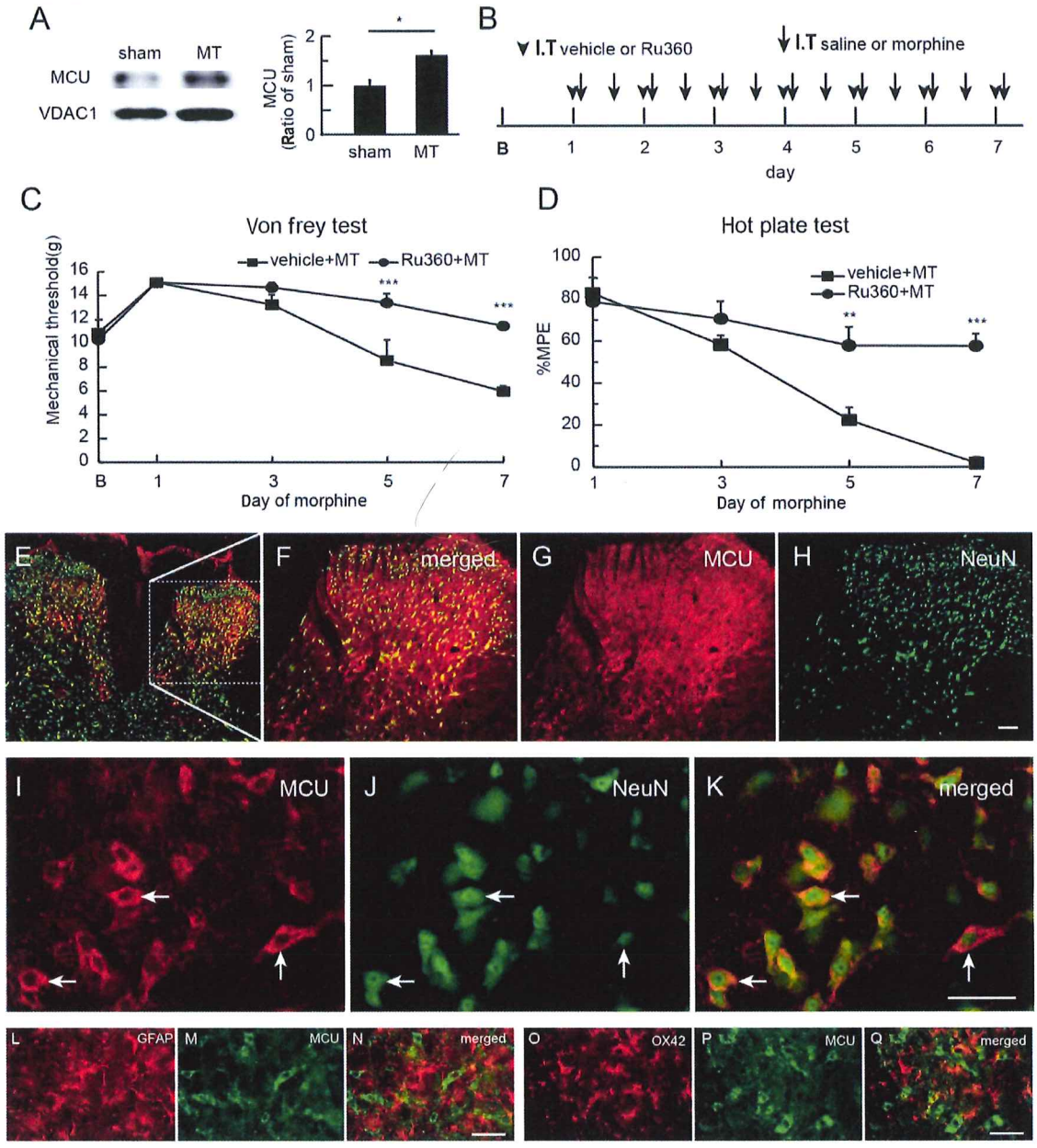

Fig. 1. Effect of mitochondrial calcium uniporter (MCU) inhibition on morphine tolerance. (a) We harvested spinal cord dorsal horn (SCDH) 1 h after the last morphine dose on Day 7 in morphine-tolerant rats. Western blots demonstrated that morphine tolerance increased the expression of MCU in the SCDH compared with sham ($P<0.05$; *t*-test; $n=5–6$). (b) Scheme for intrathecal administration. Morphine tolerance was induced by intrathecal injection of morphine (arrow; twice a day); sham group was saline. Ruthenium 360 (Ru360) or vehicle (arrowhead) was administered every morning 30 min before morphine or saline (sham). (c) Intrathecal MCU inhibitor, Ru360, significantly up-regulated the mechanical withdrawal threshold compared with vehicle ($F_{(4,40)interaction}=6.62$, $P<0.001$; $F_{(4,40)main\ effect\ time}=23.51$, $P<0.0001$; $F_{(1,10)main\ effect\ treatment}=12.53$, $P<0.01$; two-way ANOVA repeated measures; $n=6$). The mechanical withdrawal threshold in the Ru360 group was higher than that in the vehicle group on Days 5 and 7 (***$P<0.001$ *vs* vehicle; two-way ANOVA Bonferroni tests). (d) In the hotplate test, there was a significant difference in maximum possible effect (MPE) (%) of thermal latency between Ru360 and saline ($F_{(3,30)interaction}=9.47$; $P<0.001$; $F_{(3,30)main\ effect\ time}=29.45$; $P<0.0001$; $F_{(1,10)main\ effect\ treatment}=25.47$; $P<0.001$; two-way ANOVA repeated measures; $n=6$). MPE (%) in the Ru360 group was higher than that for vehicle on Day 5 or 7 (**$P<0.01$; ***$P<0.001$ *vs* vehicle; two-way ANOVA Bonferroni tests). (e–h) Low magnification of MCU immunoreactivity (IR) (MCU-IR) images. (i–k) High-magnification images display that MCU-IR co-localised with NeuN, but not with (l–n) glial fibrillary acidic protein (GFAP) or (o–q) OX42; scale bar: 50 μm. MT, morphine anti-nociceptive tolerance.

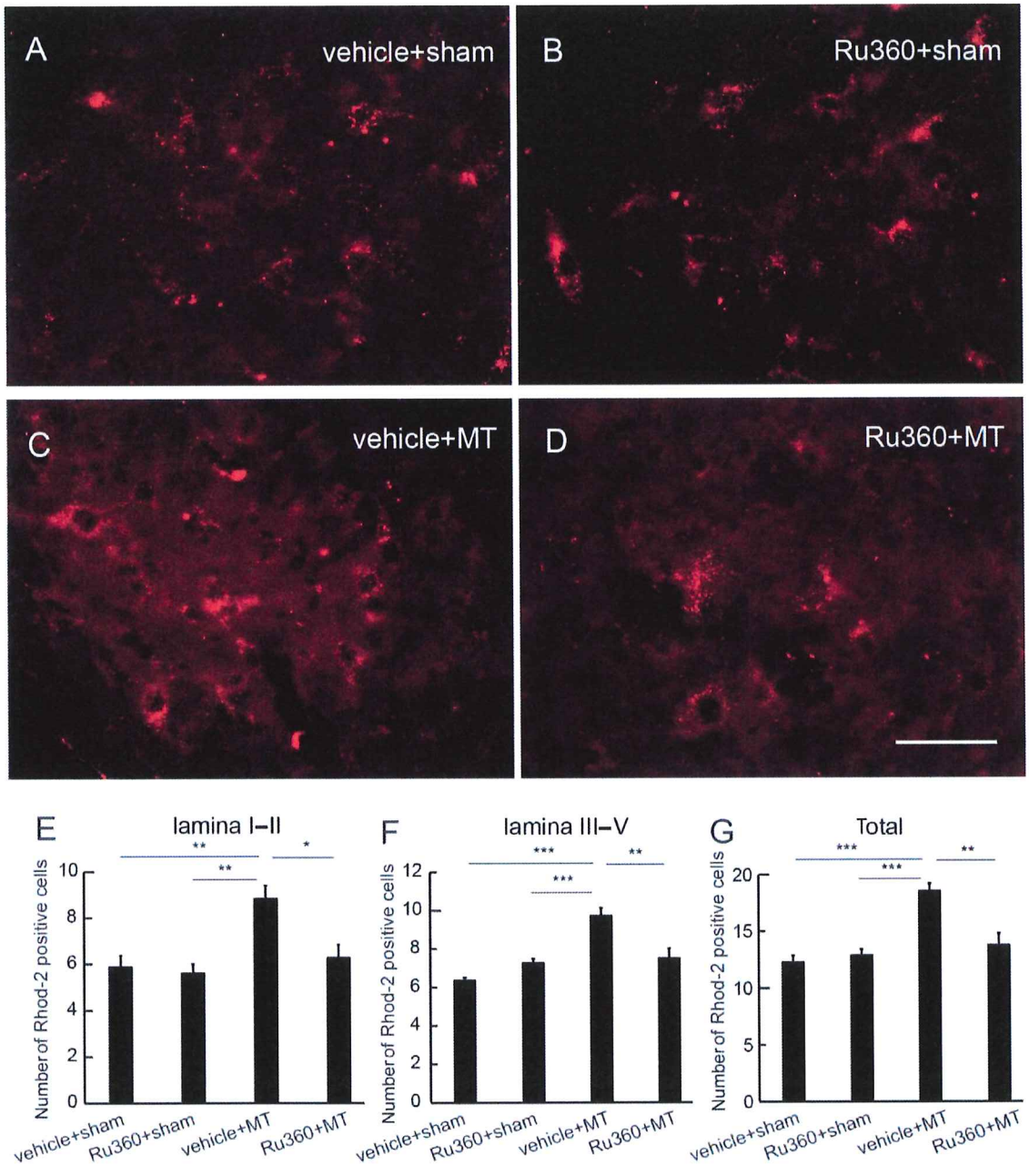

Fig. 2. Effect of mitochondrial calcium uniporter inhibition on mitochondrial calcium in spinal cord dorsal horn (SCDH) neurones. Ruthenium 360 (Ru360) (50 μM) was injected intrathecally every morning 30 min before morphine injection once a day for 7 days. At 30 min after the last morphine, Rhod-2/AM was intrathecally injected for Rhod-2 imaging. (a–d) Representative image of Rhod-2 in the SCDH in (a) saline+sham, (b) Ru360+sham, (c) saline+morphine anti-nociceptive tolerance (MT), and (d) Ru360+MT groups. (e) There was a significant increase in Rhod-2-positive cells at SCDH Laminae I and II in the vehicle+MT group compared with the vehicle+sham or Ru360+sham groups (**$P<0.01$; one-way ANOVA; $n=6$); Rhod-2-positive cells in the Ru360+MT group was lower than that in the vehicle+MT group in SCDH Laminae I and II ($P<0.05$; one-way ANOVA; $n=6$). Similarly, there was a significant increase in Rhod-2-positive cells in the vehicle+MT group compared with the vehicle+sham or Ru360+sham group in (f) Laminae III–V or (g) Laminae I–V (***$P<0.001$; one-way ANOVA; $n=6$). (f) Rhod-2-positive cells in Ru360+MT group were fewer than in the vehicle+MT group in SCDH Laminae III–V (**$P<0.01$; one-way ANOVA; $n=6$). (g) Total Rhod-2-positive cells in Laminae I–V in the Ru360+MT group was lower than in the vehicle+MT group (**$P<0.01$; one-way ANOVA; $n=6$).

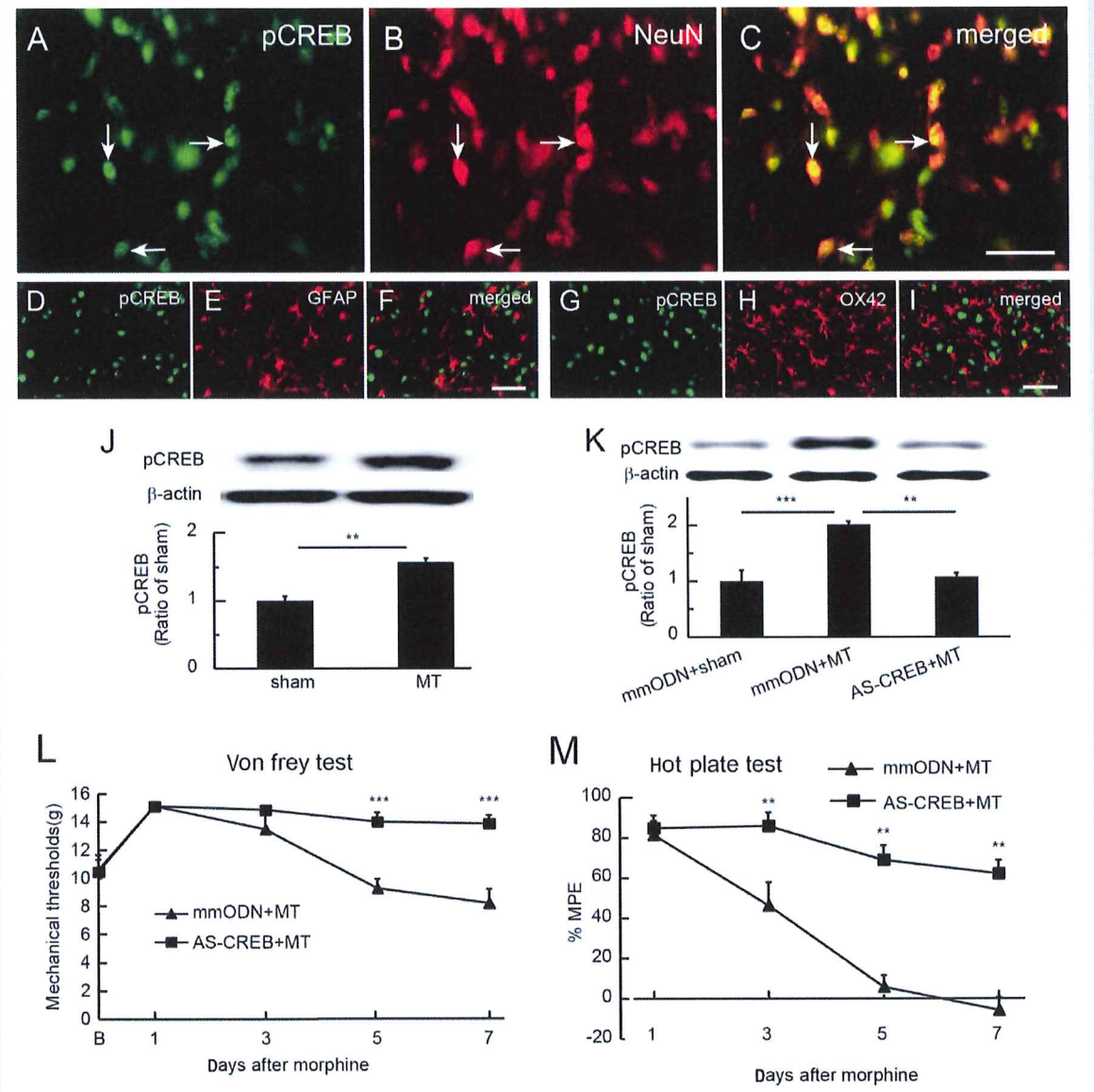

Fig. 3. Effect of knockdown of transcriptional factor, cyclic adenosine monophosphate response element (CRE)-binding protein (CREB), on spinal morphine tolerance. (a–c) Immunostaining showed that phosphorylated cyclic adenosine monophosphate response element-binding protein (pCREB) co-localised with NeuN, but not with (d–f) glial fibrillary acidic protein (GFAP) or (g–i) OX42 in spinal cord dorsal horn (SCDH) in morphine-tolerant rats, suggesting neuronal pCREB activity in morphine tolerance. (j) Western immunoblots showed that morphine tolerance up-regulated the expression of pCREB in the SCDH compared with the sham group (**P<0.01; *t*-test; n=6). (k) Expression of spinal pCREB in the mismatch ODN (mmODN)/morphine anti-nociceptive tolerance (MT) group was higher than in the sham group (***P<0.001; one-way analysis of variance [ANOVA] with *post hoc* Fisher's protected least significant difference [PLSD]; n=4–5); pCREB in the AS-CREB+MT group was significantly lower than that in the mmODN+MT group (**P<0.01; one-way ANOVA with *post hoc* Fisher's PLSD; n=4–5). (l) Intrathecal AS-CREB caused an elevation of mechanical withdrawal threshold compared with mmODN ($F_{(4,40)\text{main interaction}}$=6.70, P<0.001; $F_{(4,40)\text{main effect time}}$=15.08, P<0.0001; $F_{(1,\ 10)}$=22.93, P<0.001; two-way ANOVA repeated measures; n=6). The mechanical withdrawal threshold in the AS-CREB group was higher than in the mmODN group on Days 5 and 7 (***P<0.001 *vs* mmODN; two-way ANOVA Bonferroni tests; n=6). (m) Intrathecal AS-CREB increased %MPE in thermal latency compared with mmODN ($F_{(3,40)\text{main effect interaction}}$=9.08, P<0.001; $F_{(3,30)\text{main effect time}}$=26.41, P<0.0001; $F_{(1,\ 10)\ \text{main effect treatment}}$= 55.29, P<0.0001; two-way ANOVA repeated measures; n=6). Thermal latency in the AS-CREB group was higher than that in the mmODN group on Day 5 or 7 after ODN (**P<0.01 *vs* mmODN; two-way ANOVA Bonferroni tests; n=6).

(GFAP), OX42, NeuN, pCREB, MCU, or CPEB1 in the SCDH was performed (see Supplementary Methods and Results for details).

Mitochondrial Ca^{2+} imaging in the spinal dorsal horn

Rhod-2/AM (a mitochondrial Ca^{2+} indicator; Thermo Fisher Scientific, Waltham, MA) was dissolved in dimethylsulphoxide 2% in saline to a final concentration of 33 μM. Rhod-2 (30 μl) was injected intrathecally, as described previously[24] (see Supplementary Methods and Results for details).

Drugs

Morphine sulphate was purchased from West-Ward Pharmaceuticals (Eatontown, NJ, USA). MCU antagonist ruthenium 360 (Ru360) was purchased from VWR (Radnor, PA, USA) and dissolved in saline. The sequences of rat antisense CREB oligodeoxynucleotides (ODNs), 5′-TGGTCATCTAGTCACCGGTG-3′, and mismatch ODN (mmODN), 5′-GACCTCAGG-TAGTCGTCGTT-3′ (synthesised by Sigma-Aldrich), were designed, as reported.[25,26] The sequences of rat CPEB1 antisense ODN, 5′-CATACACCACTCCACCAAATAG-3′, and mmODN, 5′-AATAGAACACACCACCTGATAC-3′, were purchased from Sigma-Aldrich.

Data analysis

Behavioural data were analysed by two-way analysis of variance (ANOVA) with repeated measures subjected to Bonferroni testing. Statistical significance was determined by t-test or one-way ANOVA with *post hoc* test after Fisher's protected least significant difference (PLSD) (StatView 5, SAS Institute Inc., Cary, NC). Data are presented as mean (standard error of the mean), with P-values of <0.05 considered statistically significant.

Results

Role of spinal MCU in morphine tolerance

To examine the role of the MCU in morphine tolerance, we harvested SCDH after the last morphine on Day 7 for immunoblotting. Morphine tolerance increased the expression of MCU in the SCDH compared with sham; $P<0.05$; t-test; $n=5–6$ (Fig. 1a). We then examined whether MCU inhibition reduced the spinal morphine tolerance. Ru360, an MCU inhibitor, specifically blocks Ca^{2+} uptake by MCU.[27] We injected Ru360 (50 μM) intrathecally 30 min before the morning morphine injection for 7 days (Fig. 1b), and tested the mechanical threshold and thermal latency before and 60 min after the morning morphine injection on Days 1, 3, 5, and 7. Ru360 up-regulated the mechanical withdrawal threshold compared with vehicle (saline) (Fig. 1c). The mechanical withdrawal threshold in the Ru360 group was higher than in the control on Days 5 and 7 ($P<0.001$ *vs* vehicle; two-way ANOVA Bonferroni tests; $n=6$) (Fig. 1c). In the hotplate test, thermal-latency MPE was higher in the Ru360 group than that in the saline vehicle group on Day 5 or 7 ($P<0.01$, or $P<0.001$ *vs* vehicle, respectively; two-way ANOVA Bonferroni tests; $n=6$) (Fig. 1d). Neither Ru360 nor vehicle changed the basic mechanical threshold and thermal latency in control rats (Supplementary Fig. S1). The immunoreactivity (IR) of MCU in SCDH co-localised with NeuN (a neuronal marker; Fig. 1e–k), but not with GFAP (a marker of astrocytes; Fig. 1l–n) or OX42 (a marker of microglia; Fig. 1o–q), suggesting that MCU was expressed in SCDH neurones, but not glia, in morphine-tolerant rats.

MCU inhibition reduced spinal cord dorsal horn neurone mitochondrial calcium

We examined whether MCU inhibition reduced the spinal mitochondrial Ca^{2+} using a Rhod-2 assay.[24] Ru360 (50 μM) was injected intrathecally every morning 30 min before the morphine injection for 7 days. Half an hour after the last morphine dose, Rhod-2 was injected intrathecally, the animals were perfused 70 min after Rhod-2, and the spinal cord was harvested for imaging. Representative images of Rhod-2-positive cells in vehicle+sham, Ru360+sham, vehicle+morphine anti-nociceptive tolerance (MT), or Ru360+MT are shown in Fig 2. There was a significant increase in Rhod-2-positive cell number in SCDH Laminae I and II in the vehicle+MT group compared with that in the vehicle+sham or Ru360+sham groups ($P<0.01$; one-way ANOVA; Fig. 2e); Rhod-2-positive cells in the Ru360+MT group were lower than in the vehicle+MT SCDH Laminae I and II ($P<0.05$; one-way ANOVA; Fig. 2e). Similarly, there was an increase in Rhod-2-positive cells in SCDH Laminae III–V (Fig. 2f) and total amount of Rhod-2-positive cells in Laminae I–V (Fig. 2g) in the vehicle+MT group compared with the vehicle+sham or Ru360+sham group. There were fewer Rhod-2-positive cells in the Ru360+MT group than in the vehicle+MT group in Laminae III–V (Fig. 2f) or in total Rhod-2-positive cells in Laminae I–V (Fig. 2g).

Knockdown of spinal CREB reduced morphine tolerance

Chronic morphine exposure increases pCREB expression in various brain regions.[10] Immunostaining showed that spinal pCREB co-localised with NeuN (Fig. 3a–c), but not with GFAP (Fig. 3d–f) or OX42 (Fig. 3g–i), in morphine-tolerant rats. Western immunoblots showed that the expression of pCREB was up-regulated in the SCDH in the morphine tolerant compared with the sham group; $P<0.01$; t-test; $n=6$ (Fig. 3j). To determine if knockdown of CREB using antisense ODN against CREB (AS-CREB; 50 μg) reduced the spinal morphine tolerance, we intrathecally administered AS-CREB or mmODN 30 min before each morning morphine injection for 7 days. Using western immunoblots, we found that spinal pCREB in the mmODN+MT group was higher than in the sham group; $P<0.001$; one-way ANOVA with *post hoc* Fisher's PLSD; $n=4–5$ (Fig. 3k); in the AS-CREB+MT group, pCREB was lower than in the mmODN+MT group; $P<0.01$; one-way ANOVA with *post hoc* Fisher's PLSD; $n=4–5$ (Fig. 3k). We tested the mechanical threshold and thermal latency 60 min after morphine injection on Days 1, 3, 5, and 7. Intrathecal AS-CREB caused an elevation of mechanical threshold compared with mmODN (Fig. 3l). The mechanical threshold in the AS-CREB group was higher than that in the mmODN group on Days 5 and 7; $P<0.001$ *vs* mmODN; two-way ANOVA Bonferroni tests; $n=6$ (Fig. 3l). Intrathecal AS-CREB increased MPE in thermal latency compared with mmODN (Fig. 3m). Thermal latency in the AS-CREB group was higher than in the mmODN group on

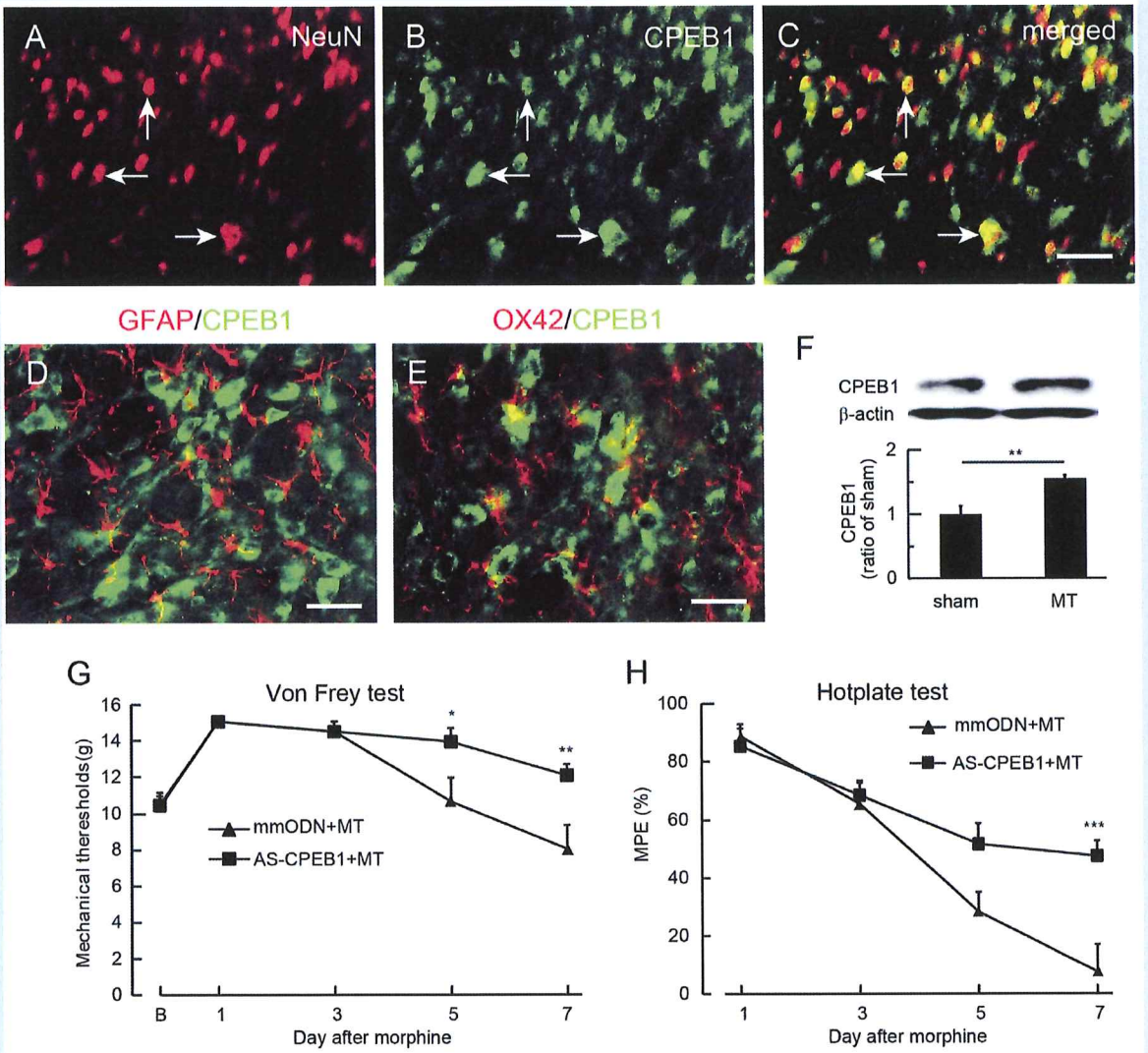

Fig. 4. Effect of spinal cytoplasmic polyadenylation element-binding protein 1 (CPEB1) on morphine tolerance. Double immunostaining showed that the immunoreactivity (IR) of CPEB1-IR co-localised with (a–c) NeuN, but not with (d) glial fibrillary acidic protein (GFAP) or (e) OX42. (f) Western immunoblots showed that morphine tolerance increased the expression of CPEB1 in the spinal cord dorsal horn compared with sham (**P<0.01; t-test; n=4). (g) Intrathecal AS-CPEB1 caused an elevation of mechanical withdrawal threshold compared with mismatch oligodeoxynucleotide (mmODN) ($F_{(4,40)interaction}$=4.30, P<0.01; $F_{(4,40)\ main\ effect\ time}$=22.13, P<0.0001; $F_{(1,10)\ main\ effect\ treatment}$=5.27, P<0.05; two-way analysis of variance [ANOVA] repeated measures). The mechanical withdrawal threshold in the AS-CPEB1+morphine anti-nociceptive tolerance (MT) group was higher than in the mmODN+MT group 5 and 7 days after ODN (*P<0.05, ** P<0.01 *vs* mmODN+MT; two-way ANOVA Bonferroni tests). (h) Intrathecal AS-CPEB1 increased thermal latency using hotplate test compared with mmODN $F_{(3,30)interaction}$=5.90, P<0.01; $F_{(3,30)\ main\ effect\ time}$=43.68, P<0.0001; $F_{(1,10)main\ effect\ treatment}$=6.78, P<0.05; two-way ANOVA repeated measures). The mechanical withdrawal threshold in the AS-CPEB1+MT group was higher than in the mmODN+MT group on Day 7 (***P<0.001 *vs* mmODN+MT; two-way ANOVA Bonferroni tests).

Day 5 or 7; P<0.01 *vs* mmODN; two-way ANOVA Bonferroni tests; n=6 (Fig. 3m). In sham rats receiving repeatedly intrathecal saline for 7 days, there was no significant difference between intrathecal mmODN and AS-CREB injections on basic mechanical threshold and thermal latency (Supplementary Fig. S2).

Role of spinal CPEB in morphine tolerance

CPEB is a sequence-specific RNA-binding protein at the mRNA 3′ untranslated region (UTR) regulating mRNA translation that modulates neuronal synaptic plasticity.[28] CPEB is responsible for induction of hyperalgesia priming in the chronification of

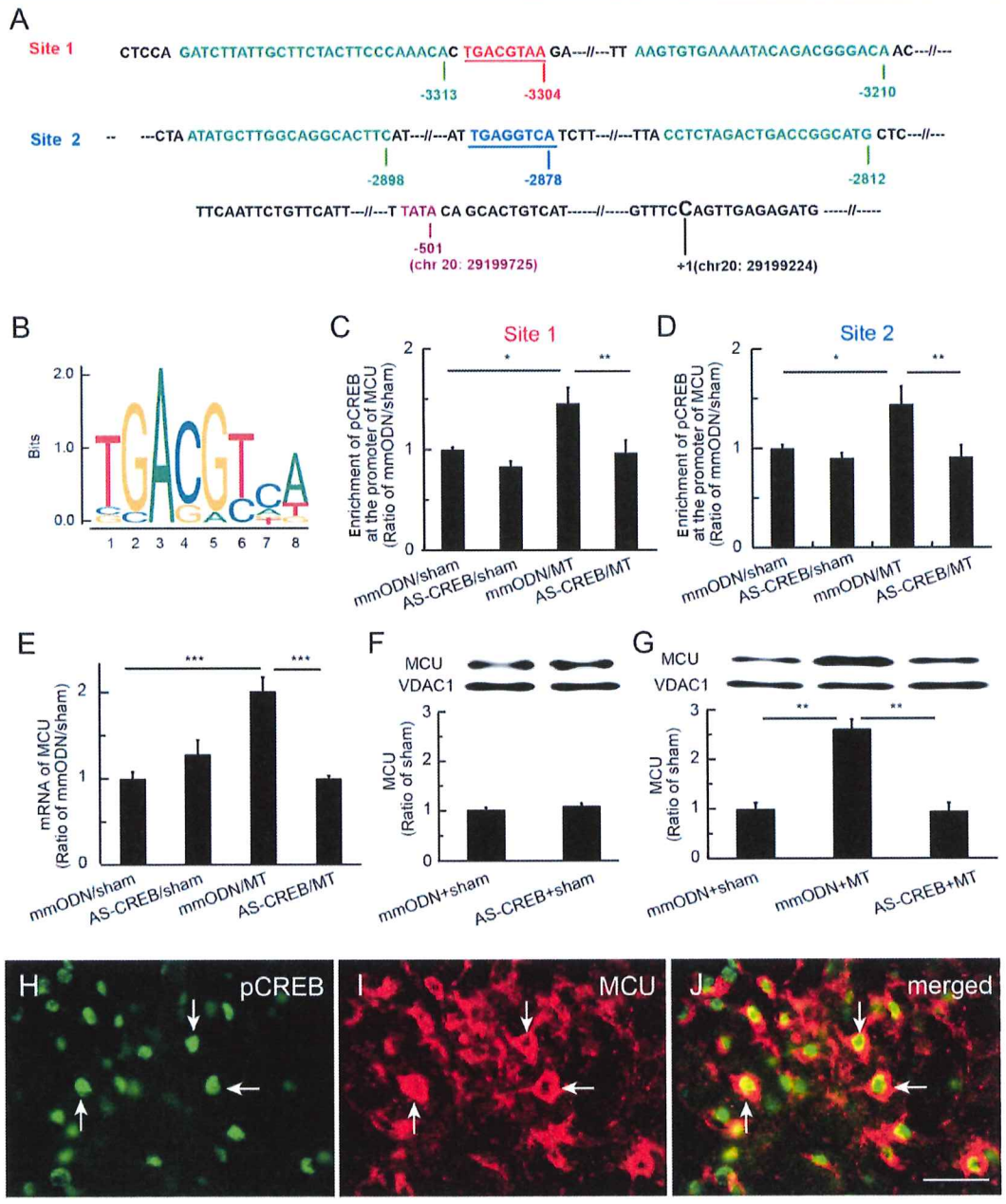

Fig. 5. Phosphorylated cyclic adenosine monophosphate response element-binding protein (pCREB) bound *mcu* gene promoter regions in the spinal cord dorsal horn (SCDH) and mediated mitochondrial calcium uniporter (MCU) transcription. (a) We analysed the alignment of rat MCU gene promoter regions, and found two putative CRE-binding areas, Site 1 (TGACGTAA)[29] and Site 2 (TGAGGTCA),[30,31] and chromatin immunoprecipitation with quantitative PCR (ChIP-qPCR) primer areas of the MCU gene at rat chromosome 20 (accession number: NC_005119; NCBI Reference Sequence: NC_005119.4). The TATA box of *mcu* gene was shown. The first base C (chr 20: 29199224) of the first intron of the *mcu* gene was referred to as number +1. (b) Motif of the CREB-binding sites based on the JASPAR data sets (http://jaspar.genereg.net/matrix/MA0018.2). (c and d) ChIP-qPCR assay showed that enrichment of pCREB at CRE Site 1 or 2 of the *mcu* gene promoter region in the mismatch oligodeoxynucleotide (mmODN)+morphine anti-nociceptive tolerance (MT) group was increased compared with the mmODN+sham group (*P<0.05; one-way analysis of variance [ANOVA]; n=5). Enrichment of pCREB at Site 1 or 2 on *mcu* gene promoter in the AS-CREB+MT group was lower than that in the mmODN+MT group (**P<0.01; one-way ANOVA; *post hoc* Fisher's protected least significant difference [PLSD]; n=5). (e) RT–PCR showed increased MCU mRNA expression (***P<0.001; one-way ANOVA; *post hoc* Fisher's PLSD test; n=5). (f and g) Western immunoblots showed no differences in expression of MCU protein between mmODN+sham and AS-CREB+sham groups (f). (g) MCU protein expression increased (**P<0.01; one-way ANOVA). (h–j) Double immunostaining showed that pCREB was co-localised with MCU in the SCDH in morphine-tolerant rats; scale bar: 50 μm.

pain,[14] and CPEB1 is involved in anxiety and chronic pain.[18] To examine the role of CPEB in morphine tolerance, double immunostaining showed that CPEB1 IR co-localised with NeuN (Fig. 4a–c), but not with GFAP (Fig. 4d) or OX42 (Fig. 4e). Western blots showed that morphine tolerance increased the expression of CPEB1 in SCDH compared with sham treatment ($P<0.01$; t-test; $n=4$; Fig. 4f). To further verify the role of CPEB1 in morphine tolerance, we examined the effect of CPEB1 knockdown using CPEB1 antisense ODN (AS-CPEB). AS-CPEB1 or mmODN (40 μg) was injected intrathecally 30 min before each morning morphine injection for 7 days followed by testing of mechanical threshold and thermal latency 60 min after the injection on Days 1, 3, 5, and 7. Intrathecal AS-CPEB1 caused an elevation of mechanical withdrawal threshold compared with mmODN (Fig. 4g). The mechanical withdrawal threshold in the AS-CPEB1+MT group was higher than in the mmODN+MT group on Days 5 and 7 ($P<0.05$; two-way ANOVA Bonferroni tests; Fig. 4g). Intrathecal AS-CPEB increased MPE in the hotplate test compared with mmODN (Fig. 4h). Thermal MPE in the AS-CPEB1+MT group was higher than in the mmODN+MT group on Day 7 ($P<0.001$ *vs* mmODN+MT; two-way ANOVA Bonferroni tests; Fig. 4h). Neither AS-CPEB1 nor mmODN changed the basic mechanical threshold or thermal latency in sham rats (Supplementary Fig. S3).

pCREB binding mediated MCU transcription

The activation of pCREB induces MCU expression through binding to the *mcu* gene promoter to drive mRNA transcription in human cultured HeLa cells.[20] To further clarify the role of pCREB in mediating MCU expression in rats *in vivo*, we analysed the alignment of rat *mcu* gene promoter regions. The two putative CRE-binding areas, Site 1 (TGACGTAA)[29] and Site 2 (TGAGGTCA)[30,31]; the ChIP-qPCR primer areas of the gene at rat chromosome 20 (accession number: Genbank Location, Chromosome 20, NC_005119.4 (29037452..29199224); NCBI Reference Sequence: NC_005119.4); and the TATA box (a DNA sequence in the promoter region of genes) of the gene are shown in Fig 5a, and the motif of sequence logo for CREB-binding sites based on the JASPAR data sets (http://jaspar.genereg.net/matrix/MA0018.2) is shown in Fig 5b. We used the ChIP-qPCR assay to determine if pCREB mediated gene expression in the SCDH in an epigenetic manner. One hour after the last injection of morphine, lumbar SCDH was harvested for ChIP-qPCR, which showed that enrichment of pCREB at Site 1 or 2 on the *mcu* promoter in the mmODN+MT group was increased compared with the mmODN+sham group ($P<0.05$; one-way ANOVA; Fig. 5c and d), and that enrichment of pCREB at Site 1 or 2 in the AS-CREB+MT group was lower than in the mmODN+MT group ($P<0.01$; one-way ANOVA; Fig. 5c and d). RT–PCR revealed that MCU mRNA in the mmODN+MT group was higher than in the mmODN+-sham group, and that MCU mRNA in the AS-CREB+MT group was lower than in the mmODN+MT group (Fig. 5e). Western immunoblots showed that there was no difference in the expression of MCU protein between mmODN+sham and AS-CREB+sham groups (Fig. 5f). However, MCU protein expression in the mmODN+MT group was higher than in the mmODN+sham group; MCU in the AS-CREB+MT group was lower than in the mmODN+MT group ($P<0.01$; one-way ANOVA; Fig. 5g). These results suggest that pCREB modulates *mcu* gene expression in an epigenetic manner in morphine tolerance. Double immunostaining showed that pCREB was co-localised with MCU in the SCDH of morphine-tolerant rats (Fig. 5h–j).

CPEB1 binding to MCU mRNA 3′ UTR *in vitro*

Transcription of the *mcu* gene is mediated by pCREB binding to the *mcu* promoter in HeLa cells.[20] To verify whether CPEB1 regulates MCU mRNA translation to protein, we analysed the alignment of rat MCU mRNA 3′ UTR (immediately following the translation stop codon), and observed that there were two CPE motifs, UUUUUAAU[32] (M1) and CPE consensus sequence UUUUUAU[13,33] (M2) (Fig. 6a; Supplementary Fig. S4). Expression of MCU and CPEB1 was induced in rat neuronal B35 cells treated with recombinant TNFα for 3 h, as described.[22] Using an RNA immunoprecipitation (RNA-IP) assay, we observed that MCU mRNA expression in CPEB1 immunoprecipitates was not increased at the M1 CPE sequence (Fig. 6b); however, MCU mRNA in CPEB1 immunoprecipitates was increased at the M2 CPE consensus sequence (Fig. 6c). We verified that expression of MCU and CPEB1 proteins was up-regulated by rTNFα treatment (Supplementary Fig. S5).

Knockdown of spinal CPEB1 reduced the expression of spinal MCU protein in morphine tolerance

We determined the effect of spinal CPEB1 knockdown by CPEB1 antisense ODN on protein expression of CPEB1 and MCU in spinal morphine tolerance. SCDH was collected on Day 7 at 1 h after the last morphine injection for western immunoblot analysis. CPEB1 expression in the mmODN+MT group increased compared with the sham group ($P<0.01$; one-way ANOVA with *post hoc* Fisher's PLSD test; $n=4–5$). Spinal CPEB1 in the AS-CPEB1+MT group was lower than in the mmODN+MT group ($P<0.05$; one-way ANOVA with *post hoc* Fisher's PLSD test; $n=4–5$; Fig. 6d). MCU protein expression was increased in the mmODN+MT group compared with the sham group treated with mmODN ($P<0.01$; one-way ANOVA with *post hoc* Fisher's PLSD; $n=4–5$; Fig. 6e). MCU in the AS-CPEB1+MT group was lower than in the mmODN+MT group ($P<0.01$; one-way ANOVA with *post hoc* Fisher's PLSD; $n=4–5$; Fig. 6e). Double immunostaining showed that CPEB1 IR co-localised with MCU (Fig. 6f).

Discussion

We found that: (i) spinal morphine tolerance increased the expression of MCU, pCREB, and CPEB1 in the SCDH; (ii) MCU inhibition decreased the behavioural response to morphine tolerance and mitochondrial Ca^{2+} accumulation; (iii) CREB or CPEB1 knockdown reduced the morphine-tolerance behavioural response; (iv) pCREB regulated the *mcu* gene transcription in an epigenetic manner; (v) CPEB1 binds MCU mRNA 3′ UTR; and (vi) knockdown of CPEB1 down-regulated the MCU protein expression. The present findings suggest that spinal MCU was regulated by pCREB and CPEB1 in spinal morphine tolerance.

Chronic use of opioid analgesics is often hampered by the development of unwanted side-effects, such as tolerance and dependence, contributing to the current epidemic of opioid abuse and overdose-related deaths.[34] The molecular mechanisms of morphine are still unclear. Chronic morphine treatment induces neuro-inflammation in a manner analogous to endotoxin.[35] Opioid-induced neurotoxic consequences involve neuronal apoptosis.[5] Chronic opioid use

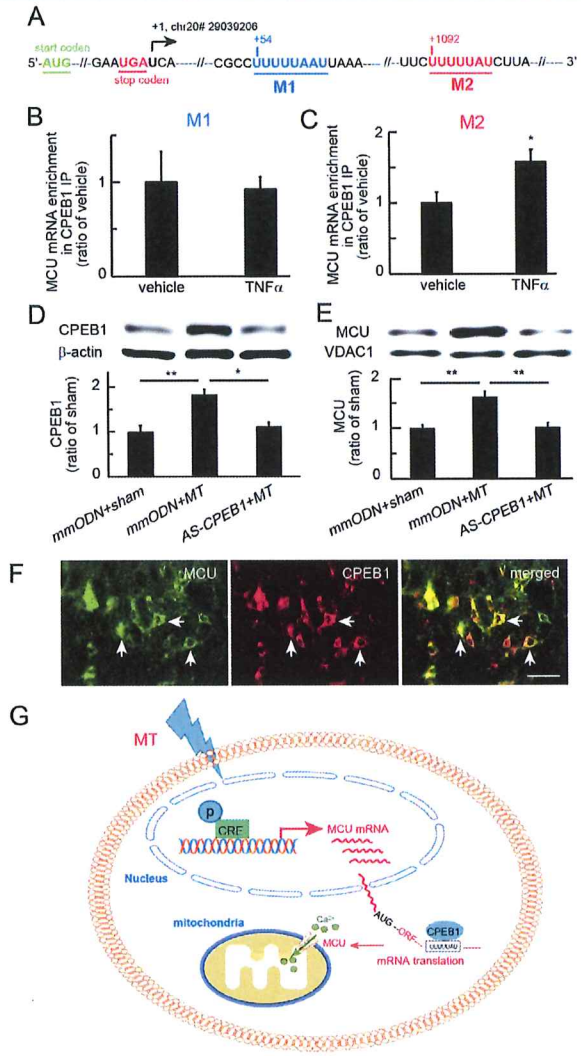

Fig. 6. Cytoplasmic polyadenylation element-binding protein 1 (CPEB1) on the mitochondrial calcium uniporter (MCU) mRNA. (a) We analysed the alignment of rat CPEB1 motifs at the MCU mRNA 3′ untranslated region (UTR) and found two putative CPE-binding areas, *motif* 1, UUUUUAAU[32] (M1), and *motif* 2, CPE consensus sequence, UUUUUAU[13,33] (M2). AUG, translation start codon, and UGA, translation stop codon, are shown. The first base U (chr20# 29039206) following UGA was referred to as number +1. (b) To induce the expression of MCU and CPEB1, we used rat neuronal B35 cells treated with recombinant tumour necrosis factor alpha (rTNFα) for 3 h. Using an RNA immunoprecipitation assay, we observed that MCU mRNA in CPEB1 immunoprecipitation was not increased at the M1 CPE sequence, and that (c) MCU mRNA in CPEB1 immunoprecipitation was increased at the M2 CPE consensus sequence. (d) Morphine-tolerant rats were treated with antisense oligodeoxynucleotide against CPEB1. Western immunoblots showed a significant increase in CPEB1 in the mismatch oligodeoxynucleotide (mmODN)+morphine anti-nociceptive tolerance (MT) group compared with the sham group (**P<0.01; one-way analysis of variance [ANOVA] with *post hoc* Fisher's protected least significant difference [PLSD] test; n=4–5). Spinal CPEB1 in the AS-CPEB1+MT group was lower than in the mmODN+MT group (*P<0.05; one-way ANOVA with *post hoc* Fisher's PLSD test; n=4–5). (e) Western immunoblots showed that MCU in the spinal cord dorsal horn (SCDH) was increased in the mmODN+MT group compared with sham rats treated with mmODN; MCU in the SCDH of the AS-CPEB+MT group was lower than in the mmODN+MT group (**P<0.01; one-way ANOVA with *post hoc* Fisher's PLSD; n=4–5). (f) Double immunostaining showed that CPEB1 immunoreactivity was co-localised with MCU; scale bar: 50 μm. (g) The proposed signalling pathways mediated by phosphorylated cyclic adenosine monophosphate response element-binding protein (pCREB) and CPEB1. Morphine tolerance evoked neuronal activity to induce phosphorylation of CREB. pCREB binds to CRE sites of the *mcu* gene promoter to induce MCU transcriptional expression. Up-regulated CPEB1 may regulate MCU translation. CPE motifs in MCU mRNA 3′ UTRs reside in a complex containing CPEB1.[13] CPEB1 binds to the MCU mRNA 3′ UTR to regulate MCU mRNA translation. AUG, mRNA translation start codon; ORF, open reading frame of the stretch of codons between AUG and a stop codon.

often leads to altered gene activation and increased oxidative stress affecting protein expression and ion channel function. N-methyl-D-aspartate receptor-mediated activation of intracellular signalling may also be involved in the development of opioid tolerance.[36] Spinal reactive oxygen species contribute to chronic morphine effects.[37,38] Emerging evidence suggests a critical role for epigenetic mechanisms in opioid abuse.[12] Gene transcriptional factors play a pivotal role in learning, memory, and drug abuse.[12,39] Chronic morphine induced the upregulation of spinal pCREB.[36] However, the molecular modulation at specific genes in spinal morphine tolerance is still not clear.

Mitochondrial Ca^{2+} is involved in many functions from control of metabolism and ATP production to regulation of cell death. The activity of the MCU as a highly selective ion channel controls the mitochondrial Ca^{2+} influx.[40] MCU, which was identified genetically in 2011,[41,42] enhances mitochondrial Ca^{2+} uptake upon overexpression.[42] We observed that the MCU inhibitor, Ru360, reduced the behavioural response to morphine tolerance. Consistent with MCU expression controlling mitochondrial Ca^{2+} uptake in cultured cells[20] and in mouse SCDH,[24] we used Rhod-2/AM (a mitochondrial Ca^{2+} indicator) fluorescence assay to show that morphine tolerance increased the Ca^{2+} accumulation in mitochondria, and that intrathecal Ru360 decreased the mitochondrial Ca^{2+} in morphine-tolerant rats, the first demonstration of a role of MCU in morphine tolerance.

CREB is involved in learning, memory, and drug addiction,[43] and is thought to be an important mediator in chronic morphine treatment.[44,45] The number of neurones expressing pCREB is increased in morphine-exposed cultured neurones, and in morphine-tolerant rats the number of pCREB-expressing neurones in the lumbar dorsal horn ganglion is also increased.[11] Previous studies showed that morphine tolerance increased pCREB in the spinal cord.[46,47] We found that chronic morphine treatment increased pCREB in the SCDH in line with these findings.[46,47]

CPEB plays an important role in modulating synaptic plasticity, learning, and memory.[28] Polyadenylation of mRNA initiates translation, which is regulated by CPEB.[28,48] CPEB plays an important role in the induction of hyperalgesic priming, raising the possibility of a role in the chronification of pain.[14] The CPEB family of RNA-binding proteins is composed of four members in vertebrates (CPEB1–4). CPEB1 is essential to the regulation of mitochondrial energy production in neurones,[13] and stabilises the binding of activated cytoplasmic polyadenylation specific factor that attracts poly(A) polymerase to catalyse poly(A) elongation. The polyadenylated poly(A) tail is involved in the activation of protein translation. Knockdown of CPEB expression by intrathecal antisense ODN can prevent the induction of hyperalgesic priming,[49] and a similar mechanism is shared in chronic opioid treatment.[50] We found that chronic morphine tolerance increased the expression of CPEB1 in SCDH neurones, and that knockdown of CPEB1 reduced morphine tolerance, which is consistent with previous studies showing that CPEB1 is involved in hypernociception.[14]

Protein expression is controlled by extensive transcriptional or translational processing. Recent studies have implicated epigenetic modulation in brain reward regions after drug abuse or stress.[51] However, little is known about MCU regulation through gene transcription and translation in morphine tolerance. CREB phosphorylation modulates gene transcription that is dependent on the activation of CRE at the promoters.[52] In human HeLa cells, CREB binds the *mcu* gene promoter and initiates gene transcription.[20] Our bioinformatic analysis revealed at least two putative CREB-binding sites in the rat *mcu* promoter location, and we found that morphine tolerance increased the enrichment of pCREB on *mcu* gene promoter regions, which was reduced by knockdown of CREB, suggesting that pCREB regulates *mcu* gene transcription.

CPEB1 is a sequence-specific mRNA-binding protein that controls mRNA translation to protein.[53] CPEB binds CPE, a uridine-rich sequence element (consensus UUUUUAU motif) of the 3′ UTR of target mRNAs.[33,54] We found that MCU mRNA contains CPEs in its 3′ UTR and that CPEB1 was enriched on the MCU mRNA 3′ UTR in the cultured neurones, suggesting that CPEB1 mediates MCU mRNA translation and increases MCU protein expression. Knockdown of CPEB1 expression prevented the up-regulation of MCU protein, suggesting that CPEB1 plays an important role of MCU translation. However, the detailed mechanism of CPEB1 regulation of MCU translation is still unclear.

In conclusion, we provide evidence that spinal morphine tolerance increased MCU, pCREB, and CPEB1; that pCREB mediated MCU expression in an epigenetic manner; and that CPEB1 likely contributed to MCU protein regulation in morphine tolerance. The results also suggest that an MCU inhibitor, or agents blocking pCREB or CPEB1 upregulation may be useful in preventing the development of opioid tolerance, an issue of significant clinical relevance.

Authors' contributions

Study conception/design: KT, HY, JG, SH.
Data acquisition: KT, HY, JG, SH, DI, SL, TI, YK.
Data analysis/interpretation: all authors.
Writing paper: KT, HY, JG, SH, CD, TK.
Approving final version of the paper: all authors.

Declaration of interest

The authors declare that they have no conflicts of interest.

Acknowledgements

Authors thank Kentaro Hayashi's assistant in preparing the paper.

Funding

National Institutes of Health (R01NS066792, DA026734, R01DA34749, R01DA047089, and R01DA047157) to SH; and the Department of Anesthesiology, University of Miami Miller School of Medicine, Miami, FL, USA.

Appendix A. Supplementary data

Supplementary data to this article can be found online at https://doi.org/10.1016/j.bja.2019.05.027.

References

1. O'Brien PL, Karnell LH, Gokhale M, Kenneth Pack BS, Campopiano M, Zur J. Prescribing of benzodiazepines and opioids to individuals with substance use disorders. *Drug Alcohol Depend* 2017; **178**: 223–30

2. Volkow ND, McLellan AT. Opioid abuse in chronic pain—misconceptions and mitigation strategies. *N Engl J Med* 2016; **374**: 1253–63
3. Frenk SM, Porter KS, Paulozzi LJ. Prescription opioid analgesic use among adults: United States, 1999–2012. *NCHS Data Brief* 2015; **1–8**
4. Miller M, Barber CW, Leatherman S, et al. Prescription opioid duration of action and the risk of unintentional overdose among patients receiving opioid therapy. *JAMA Intern Med* 2015; **175**: 608–15
5. Mao J, Sung B, Ji RR, Lim G. Neuronal apoptosis associated with morphine tolerance: evidence for an opioid-induced neurotoxic mechanism. *J Neurosci* 2002; **22**: 7650–61
6. Liu JC, Parks RJ, Liu J, et al. The in vivo biology of the mitochondrial calcium uniporter. *Adv Exp Med Biol* 2017; **982**: 49–63
7. Kim HY, Lee KY, Lu Y, et al. Mitochondrial Ca^{2+} uptake is essential for synaptic plasticity in pain. *J Neurosci* 2011; **31**: 12982–91
8. Ko SW, Wu LJ, Shum F, Quan J, Zhuo M. Cingulate NMDA NR2B receptors contribute to morphine-induced analgesic tolerance. *Mol Brain* 2008; **1**: 2
9. Barrot M, Olivier JD, Perrotti LI, et al. CREB activity in the nucleus accumbens shell controls gating of behavioral responses to emotional stimuli. *Proc Natl Acad Sci U S A* 2002; **99**: 11435–40
10. Ren X, Lutfy K, Mangubat M, et al. Alterations in phosphorylated CREB expression in different brain regions following short- and long-term morphine exposure: relationship to food intake. *J Obes* 2013; **2013**: 764742
11. Ma W, Zheng WH, Powell K, Jhamandas K, Quirion R. Chronic morphine exposure increases the phosphorylation of MAP kinases and the transcription factor CREB in dorsal root ganglion neurons: an in vitro and in vivo study. *Eur J Neurosci* 2001; **14**: 1091–104
12. Koo JW, Mazei-Robison MS, LaPlant Q, et al. Epigenetic basis of opiate suppression of Bdnf gene expression in the ventral tegmental area. *Nat Neurosci* 2015; **18**: 415–22
13. Ivshina M, Lasko P, Richter JD. Cytoplasmic polyadenylation element binding proteins in development, health, and disease. *Annu Rev Cell Dev Biol* 2014; **30**: 393–415
14. Bogen O, Alessandri-Haber N, Chu C, Gear RW, Levine JD. Generation of a pain memory in the primary afferent nociceptor triggered by PKCepsilon activation of CPEB. *J Neurosci* 2012; **32**: 2018–26
15. Ferrari LF, Bogen O, Alessandri-Haber N, Levine E, Gear RW, Levine JD. Transient decrease in nociceptor GRK2 expression produces long-term enhancement in inflammatory pain. *Neuroscience* 2012; **222**: 392–403
16. Ferrari LF, Bogen O, Levine JD. Role of nociceptor αCaMKII in transition from acute to chronic pain (hyperalgesic priming) in male and female rats. *J Neurosci* 2013; **33**: 11002–11
17. Zhang JH, Panicker LM, Seigneur EM, et al. Cytoplasmic polyadenylation element binding protein is a conserved target of tumor suppressor HRPT2/CDC73. *Cell Death Differ* 2010; **17**: 1551–65
18. Yue J, Wang XS, Guo YY, et al. Anxiolytic effect of CPEB1 knockdown on the amygdala of a mouse model of inflammatory pain. *Brain Res Bull* 2018; **137**: 156–65
19. Mayer DJ, Mao J, Holt J, Price DD. Cellular mechanisms of neuropathic pain, morphine tolerance, and their interactions. *Proc Natl Acad Sci U S A* 1999; **96**: 7731–6
20. Shanmughapriya S, Rajan S, Hoffman NE, et al. Ca^{2+} signals regulate mitochondrial metabolism by stimulating CREB-mediated expression of the mitochondrial Ca^{2+} uniporter gene MCU. *Sci Signal* 2015; **8**: ra23
21. Zheng W, Ouyang H, Zheng X, et al. Glial TNFα in the spinal cord regulates neuropathic pain induced by HIV gp120 application in rats. *Mol Pain* 2011; **7**: 40
22. Yi H, Liu S, Kashiwagi Y, et al. Phosphorylated CCAAT/enhancer binding protein beta contributes to rat HIV-related neuropathic pain, in vitro and in vivo studies. *J Neurosci* 2018; **38**: 555–74
23. Hao S, Liu S, Zheng X, et al. The role of TNFα in the periaqueductal gray during naloxone-precipitated morphine withdrawal in rats. *Neuropsychopharmacology* 2011; **36**: 664–76
24. Kim HY, Lee KY, Lu Y, et al. Mitochondrial Ca^{2+} uptake is essential for synaptic plasticity in pain. *J Neurosci* 2011; **31**: 12982–91
25. Ma W, Hatzis C, Eisenach JC. Intrathecal injection of cAMP response element binding protein (CREB) antisense oligonucleotide attenuates tactile allodynia caused by partial sciatic nerve ligation. *Brain Res* 2003; **988**: 97–104
26. Ferrari LF, Bogen O, Reichling DB, Levine JD. Accounting for the delay in the transition from acute to chronic pain: axonal and nuclear mechanisms. *J Neurosci* 2015; **35**: 495–507
27. Nguyen NX, Armache JP, Lee C, et al. Cryo-EM structure of a fungal mitochondrial calcium uniporter. *Nature* 2018; **559**: 570–4
28. Richter JD. CPEB: a life in translation. *Trends Biochem Sci* 2007; **32**: 279–85
29. Taupenot L, Mahata SK, Wu H, O'Connor DT. Peptidergic activation of transcription and secretion in chromaffin cells. Cis and trans signaling determinants of pituitary adenylyl cyclase-activating polypeptide (PACAP). *J Clin Invest* 1998; **101**: 863–76
30. Ikuyama S, Shimura H, Hoeffler JP, Kohn LD. Role of the cyclic adenosine 3′,5′-monophosphate response element in efficient expression of the rat thyrotropin receptor promoter. *Mol Endocrinol* 1992; **6**: 1701–15
31. Berhane K, Boggaram V. Identification of a novel DNA regulatory element in the rabbit surfactant protein B (SP-B) promoter that is a target for ATF/CREB and AP-1 transcription factors. *Gene* 2001; **268**: 141–51
32. Paris J, Richter JD. Maturation-specific polyadenylation and translational control: diversity of cytoplasmic polyadenylation elements, influence of poly(A) tail size, and formation of stable polyadenylation complexes. *Mol Cell Biol* 1990; **10**: 5634–45
33. Fox CA, Sheets MD, Wickens MP. Poly(A) addition during maturation of frog oocytes: distinct nuclear and cytoplasmic activities and regulation by the sequence UUUUUAU. *Genes Dev* 1989; **3**: 2151–62
34. Cheatle MD. Prescription opioid misuse, abuse, morbidity, and mortality: balancing effective pain management and safety. *Pain Med* 2015; **16**. S3–8
35. Wang X, Loram LC, Ramos K, et al. Morphine activates neuroinflammation in a manner parallel to endotoxin. *Proc Natl Acad Sci U S A* 2012; **109**: 6325–30
36. Lim G, Wang S, Zeng Q, Sung B, Yang L, Mao J. Expression of spinal NMDA receptor and PKCγ after chronic morphine is regulated by spinal glucocorticoid receptor. *J Neurosci* 2005; **25**: 11145–54

37. Doyle T, Bryant L, Muscoli C, et al. Spinal NADPH oxidase is a source of superoxide in the development of morphine-induced hyperalgesia and antinociceptive tolerance. *Neurosci Lett* 2010; **483**: 85–9
38. Muscoli C, Cuzzocrea S, Ndengele MM, et al. Therapeutic manipulation of peroxynitrite attenuates the development of opiate-induced antinociceptive tolerance in mice. *J Clin Invest* 2007; **117**: 3530–9
39. Nestler EJ. Common molecular and cellular substrates of addiction and memory. *Neurobiol Learn Mem* 2002; **78**: 637–47
40. Kirichok Y, Krapivinsky G, Clapham DE. The mitochondrial calcium uniporter is a highly selective ion channel. *Nature* 2004; **427**: 360–4
41. Baughman JM, Perocchi F, Girgis HS, et al. Integrative genomics identifies MCU as an essential component of the mitochondrial calcium uniporter. *Nature* 2011; **476**: 341–5
42. De Stefani D, Raffaello A, Teardo E, Szabo I, Rizzuto R. A forty-kilodalton protein of the inner membrane is the mitochondrial calcium uniporter. *Nature* 2011; **476**: 336–40
43. Ko SW, Jia Y, Xu H, et al. Evidence for a role of CaMKIV in the development of opioid analgesic tolerance. *Eur J Neurosci* 2006; **23**: 2158–68
44. Lane-Ladd SB, Pineda J, Boundy VA, et al. CREB (cAMP response element-binding protein) in the locus coeruleus: biochemical, physiological, and behavioral evidence for a role in opiate dependence. *J Neurosci* 1997; **17**: 7890–901
45. Guitart X, Thompson MA, Mirante CK, Greenberg ME, Nestler EJ. Regulation of cyclic AMP response element-binding protein (CREB) phosphorylation by acute and chronic morphine in the rat locus coeruleus. *J Neurochem* 1992; **58**: 1168–71
46. Li X, Clark JD. Morphine tolerance and transcription factor expression in mouse spinal cord tissue. *Neurosci Lett* 1999; **272**: 79–82
47. Fakurazi S, Rahman SA, Hidayat MT, Ithnin H, Moklas MA, Arulselvan P. The combination of mitragynine and morphine prevents the development of morphine tolerance in mice. *Molecules* 2013; **18**: 666–81
48. Villalba A, Coll O, Gebauer F. Cytoplasmic polyadenylation and translational control. *Curr Opin Genet Dev* 2011; **21**: 452–7
49. Ferrari LF, Bogen O, Levine JD. Nociceptor subpopulations involved in hyperalgesic priming. *Neuroscience* 2010; **165**: 896–901
50. Araldi D, Ferrari LF, Levine JD. Hyperalgesic priming (type II) induced by repeated opioid exposure: maintenance mechanisms. *Pain* 2017; **158**: 1204–16
51. Heller EA, Hamilton PJ, Burek DD, et al. Targeted epigenetic remodeling of the Cdk5 gene in nucleus accumbens regulates cocaine- and stress-evoked behavior. *J Neurosci* 2016; **36**: 4690–7
52. Carlezon Jr WA, Duman RS, Nestler EJ. The many faces of CREB. *Trends Neurosci* 2005; **28**: 436–45
53. Afroz T, Skrisovska L, Belloc E, Guillen-Boixet J, Mendez R, Allain FH. A fly trap mechanism provides sequence-specific RNA recognition by CPEB proteins. *Genes Dev* 2014; **28**: 1498–514
54. Hake LE, Mendez R, Richter JD. Specificity of RNA binding by CPEB: requirement for RNA recognition motifs and a novel zinc finger. *Mol Cell Biol* 1998; **18**: 685–93

Handling editor: H.C. Hemmings Jr

SUPPLEMENTARY METHODS AND RESULTS

Intrathecal catheter implantation and induction of morphine tolerance

In order to intrathecally deliver drugs, an intrathecal catheter (a polyethylene, PE-10) was implanted under isoflurane anaesthesia as previously described[1]. Briefly, the catheter through an incision in the atlanto-occipital membrane, was advanced 8.5 cm caudally to position its tip at the level of the lumbar enlargement. The rostral tip of the catheter was externalized on top of the skull, and sealed with a stainless steel plug. Rats were used within 5 days after implantation of the catheter. Animals showing neurological deficits after implantation were excluded. An experienced researcher carried out the surgery. Rats were injected intrathecally with saline (10 μl, sham group) or morphine (10 μg per 10 μl, MT group) twice daily for 7 consecutive days. Behavioural testing was carried out by a blinded operator to drug treatment.

Mechanical threshold

To determine mechanical withdrawal threshold, we used calibrated von Frey filaments (Stoelting, Wood Dale, IL) serially to the hind paw in ascending order of strength. In the morning of the test day, rats were placed in non-transparent plastic cubicles on a mesh floor for an acclimatization period of at least 30 min. A positive response was defined as a rapid withdrawal and/or licking of the paw immediately on application of the stimulus. Whenever there was a positive response to the stimulus, the next smaller von Frey hair was applied; whenever there was a negative response, the next higher force was applied. Rats were assigned to the cutoff value at a pressure of 15.1 g in the absence of a response. Mechanical withdrawal threshold was calculated following the method described previously with a tactile stimulus producing a 50% likelihood of withdrawal determined by using the up-and-down method [2, 3].

Hot plate test

Hot-plate thermal latency was measured with a hot plate apparatus (IITC Life Science Inc., Woodland Hills, CA). Rats were kept inside a circular transparent plastic cage on the hot plate (51 ± 0.3°C). Licking or shaking the hind paw or jumping was considered as a sign of thermal nociceptive response. Time to the first reaction was measured. The cutoff time was set to 30 s to avoid tissue damage. The antinociceptive effects of morphine were represented as a percentage of maximum possible effect (% MPE) using the formula % MPE = [(Test-Baseline)/(Cutoff-Baseline)] × 100%.

Quantitative RT-PCR

The rat lumbar L4/5 SCDH tissues were collected, and RNAeasy mini kit (Qiagen, Germantown, MD) was used for total RNA isolation. One μg of RNA was converted into the first strain of cDNA using Superscript VILO master mix (Invitrogen, Grand Island, NY), and then real time PCR was performed with Fast SYBR green master mix (Applied Biosystem, Grand Island, NY). For real time PCR, following primers were used: MCU forward 5'-CTTGCCTACATGGCCACACA-3', and reverse 5'-AGGTGACCGGTTCCATGATG-3', (accession number, NM_001106398.1); and GAPDH forward 5'-CAGGGCTGCCTTCTCTTGTG-3' and reverse 5'-AACTTGCCGTGGGTAGAGTC-3' (accession number, NM_017008.4). Specificity of the PCR product was confirmed by running agarose gel electrophoresis. All reaction data were calculated with $2^{-\Delta Ct}$ values and normalized with GAPDH.

Chromatin immunoprecipitation with quantitative PCR (ChIP-qPCR)

The SCDH tissues were homogenized and fixed with 1 % formaldehyde for 10 min, and 2.5 M glycine was used to stop the reaction. Fixed tissue was washed and re-suspended with 250 µl of SDS lysis buffer (50 mM Tris-HCL (pH 8.0), 10 mM EDTA, 1% SDS). Samples were sonicated to shear the chromatin to the size of 200-1000bp length. Size of the sheared chromatin was confirmed by running 1.5% agarose gel. Ten µl from the supernatant was taken as "input" and save it at - 20 °C. For immunoprecipitation, 15 µg of sonicated chromatin was diluted in 0.5 mL ChIP dilution buffer, and then ChIP antibody, pCREB (cat # 06-519, Millipore, Billerica, MA) for spinal cord, was added to samples. Samples were incubated, and then 20 µl protein G magnetic beads (cat # 88848, Life Technologies, Carlsbad, CA) were added and incubated additional 2 hours at 4 °C. After washes, both immunoprecipitated and input samples were incubated with Proteinase K (Sigma, St. Louis, MO) at 62 °C for 2 hours to free DNA. DNA was purified using Gene Elute PCR cleanup kit (Sigma, St. Louis, MO). Immunoprecipitated and input DNA were analyzed by quantitative PCR analysis with SYBR Green. The primers of MCU gene promoter regions were used to amplify the segment including the CRE, site 1: forward, 5'- GATCTTATTGCTTCTACTTCCCAAACA-3', reverse, 5'-TGTCCCGTCTGTATTTTCACACTT-3'; site 2: forward, 5'-ATATGCTTGGCAGGCACTTC-3', reverse, 5'- CATGCCGGTCAGTCTAGAGG -3'. All reaction data were calculated with $2^{-\Delta Ct}$ values, and the value of pCREB immunoprecipitated DNA as a percentage of the input control was calculated. The final values were converted as ratio of sham or saline group.

RNA immunoprecipitation (RIP) and qRT-PCR

B35 cells were treated with rTNFα (10 ng per ml) or vehicle [4]. After 3 hours they were washed with PBS, cross-linked with 1% formaldehyde for 10 min at room temperature and treated with glycine as

previously described [5]. After washing twice with PBS (supplied with Protein inhibitor and RNase inhibitor), we lysed the cells in lysis buffer (20 mM HEPES pH 7.5, 1.5 mM $MgCl_2$, 150 mM NaCl, 1 % NP-40, 1mM EDTA, 10 % glycerol, 10 mM DTT, 1 mM PMSF, 1X RNase inhibitors, 1 X proteases inhibitor). Lysates were immunoprecipitated with anti-CPEB1 antibody for overnight at 4 °C. Immunoprecipitation was washed in cold lysis buffer supplemented with RNase inhibitors. We resuspended the beads in lysis buffer with 1 % SDS and proteinase K, and incubated for 30 min at 55 °C, and RNA was extracted for RT-qPCR analysis. RNA was converted into first strain of cDNA, and then real time PCR was performed with Fast SYBR green master mix (Applied Biosystem, Grand Island, NY). For the real time PCR, following primers were used: M1, forward: 5'-AAGAGACTGAGAGACCCGCT-3', reverse: 5'-GCATCCACCTGCCATGCTTT-3'

M2, forward: 5'-CTGTAGCCTGTCTTCTCCACC-3', reverse: 5'-AGGTGCCATCTGGTAAGATGAT-3'; GAPDH forward: 5'-CAGGGCTGCCTTCTCTTGTG-3', reverse: 5'-AACTTGCCGTGGGTAGAGTC-3'. Melt curves were performed to ensure that non-special products were absent. All reaction data were calculated with $2^{-\Delta Ct}$ values and normalized with GAPDH.

Western blots

B35 cells or the rat SCDH tissues were lysed, homogenized and sonicated with 1x RIPA protein lysis buffer containing protease and phosphatase inhibitor cocktail (Sigma, St. Louis, MO) as previously described [6]. Proteins (30 μg) denatured, and loaded on to 10% SDS-PAGE gel, and transferred onto a PVDF membrane. The membrane was incubated with primary antibodies overnight at 4 °C, including rabbit polyclonal anti-MCU (1:1000, ABCAM, Cambridge, MA), mouse monoclonal anti-pCREB (1:2000, Millipore, Billerica, MA), goat anti-CPEB1 (1:4000, Santa Cruz Biotechnology,

Inc. Dallas, TX), mouse anti-VDAC1 (1:4000, Santa Cruz Biotechnology, Inc. Dallas, TX), and mouse monoclonal anti-β-actin (1:8000, Sigma). The PVDF membrane was incubated with secondary antibodies at room temperature, and then developed in chemiluminescence solution (Pierce Biotechnology). Chemiluminescence values from targeted protein bands were quantified and normalized with β-actin using a ChemiDoc imaging system (Bio-Rad).

Immunohistochemistry

Immunostaining was carried out as described previously[7]. Briefly, the spinal cord cryosections were incubated with mouse anti-GFAP antibody (1:3000, G3893, Sigma, Louis, MO), rabbit anti-Iba1 antibody (1:2000, 019-19741, Wako, Richmond, VA), mouse anti-OX-42 (1:100, CBL1512, Millipore, Temecula, CA), Rabbit anti-NeuN (1:2000, , ABN78, Millipore, Temecula, CA), mouse anti-NeuN antibody (1:500, MAB377, Millipore, Temecula, CA), goat anti-CPEB antibody (1:100, SC-48983, Santa Cruz Biotechnology, Inc., Dallas, TX), mouse anti-pCREB antibody (1:200, # 05-807, Millipore Temecula, CA), rabbit anti-MCU antibody (1:100, ABCAM, Cambridge, MA). The cryosections were then incubated with complementary secondary antibodies labeled with green-fluorescent Alexa Fluor 488, or red-fluorescent Alexa Fluor 594 (1:2000, Molecular Probes, Eugene, OR) for 2 hours at room temperature. Fluorescence images were captured by a fluorescent microscopy (Fluorescent M Leica/Micro CDMI 6000B).

Mitochondrial Ca^{2+} imaging in the Spinal dorsal horn

Rhod2/AM (a mitochondrial Ca^{2+} indicator, Invitrogen) was dissolved in 2% dimethylsulfoxide (DMSO) in saline to a final concentration of 33 μM. Rhod2 (30 μl) was injected intrathecally as described previously [8]. Approximately 70 min after injection, rats were perfused intracardially with

4% 1-ethyl-3-[3-dimethylaminopropyl] carbodiimide (EDC) buffer [9], and the L4-5 segments of the spinal cord were removed, postfixed in EDC buffer for 2-4 hours, and cryoprotected with 30% sucrose for 2 days. The 35-μm sections were examined under a fluorescent microscope with a rhodamine filter. Two different regions of the dorsal horn were photographed from 3 randomly selected sections from each animal: the lateral part of lamina I-II and lamina III-V. The number of Rhod2-positive cellular profiles with distinctive nuclei (dark oval shaped space surrounded by red granules) was counted from the pictures.

Data analysis

Behavioural data were analyzed by two-way analysis of variance (ANOVA) repeated measures followed by Bonferroni tests (Prism 5.0 Graph pad, San Diego, CA). The statistical significance of the differences of neurochemical changes was determined by *t* test or one-way ANOVA *post-hoc* test following Fisher's PLSD (StatView5). All data were presented as mean±SEM, and *p*-values of less than 0.05 were considered statistically significant.

SUPPLEMENTARY FIGURES AND FIGURE LEGENDS

Supplementary Figure 1

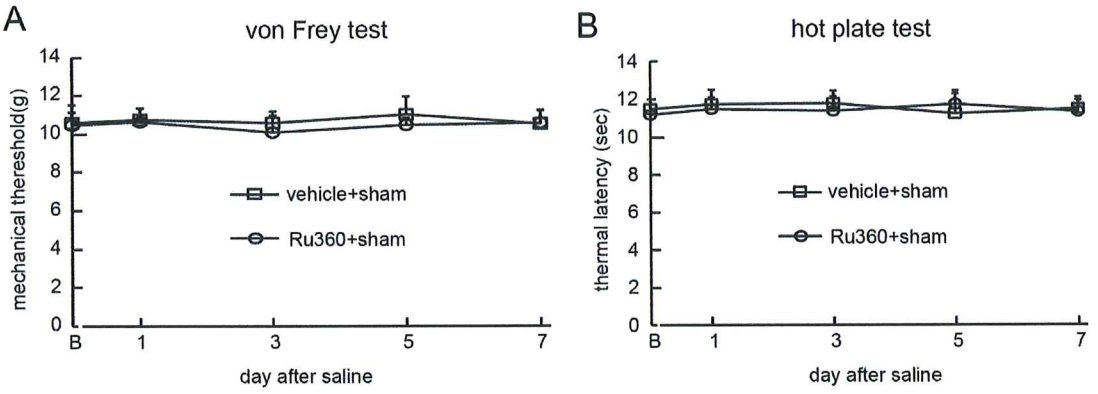

Figure S1. Effect of MCU inhibitor on mechanical threshold and thermal latency in sham rats. Neither Ru360 nor vehicle significantly changed basic mechanical threshold (A) and thermal latency (B).

Supplementary Figure 2

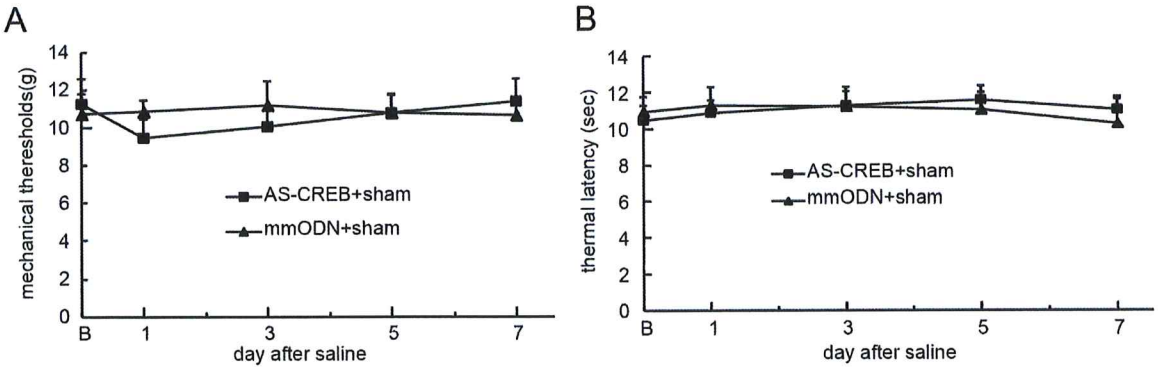

Figure S2. Effect of mmODN and AS-CREB on mechanical threshold and thermal latency in sham rats. Neither mmODN nor AS-CREB significantly changed basic mechanical threshold (A) and thermal latency (B).

Supplementary Figure S3

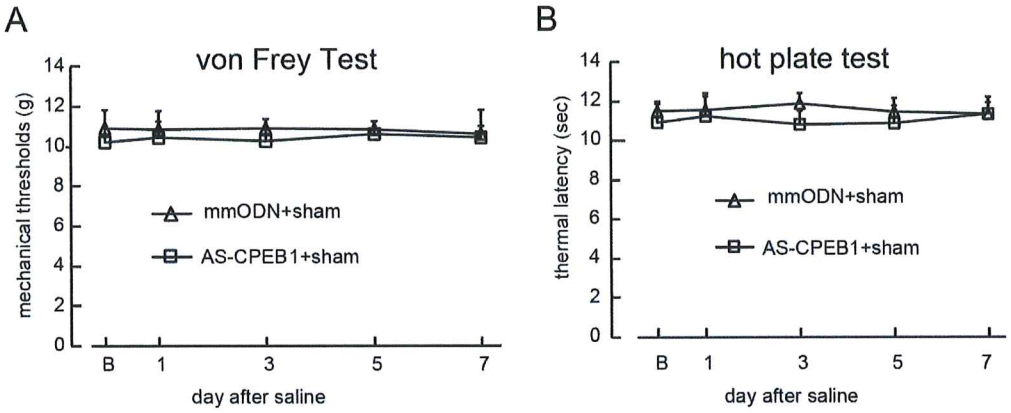

Figure S3. Effect of mmODN and AS-CPEB1 on mechanical threshold and thermal latency in sham rats. Neither AS-CPEB1 nor mmODN significantly changed basic mechanical threshold, or thermal latency in sham rats.

Supplementary Figure S4

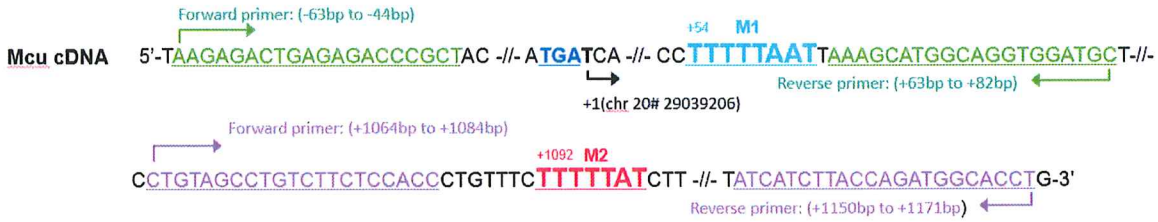

Figure S4. Scheme of CPE on *Mcu* mRNA 3' UTR, and locations of primers for RIP-PCR. The cytoplasmic polyadenylation element (CPE) attaches to the cytoplasmic polyadenylation element binding protein 1 (CPEB1). We analyzed the alignment of cDNA of MCU mRNA 3'UTR (*Chromosome 20, NC_005119.4 (29037452...29199224*). Bioinformatic analysis predicted two putative CPE motif regions at MCU mRNA 3'UTR. CPE motifs (**M1, TTTTTAAT**, blue; **M2, TTTTTAT**, red) were marked. We designed two pairs of qPCR primers for the CPE regions along the alignment. The primer locations for M1 were labelled with green colour, M2 with purple. The translation stop coden **TGA** was shown. The first base **T** following stop coden **TGA** was referred to as number +1.

Supplementary Figure S5

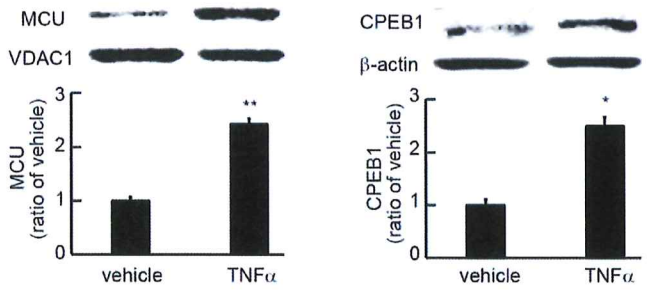

Figure S5. Expression of MCU and CPEB1 in B35 cells treated with rTNFα. To induce the expression of MCU and CPEB1, we used rat neuronal B35 cells treated with rTNFα for 3 h for neurochemical analysis as described previously[4]. The expression of MCU (*Left*) and CPEB1 (*Right*) proteins were upregulated by rTNFα treatment using western blots, * $P<0.05$, ** $P<0.01$, *t* test, n=3.

SUPPLEMENTARY REFERENCES:

1 Zheng W, Ouyang H, Zheng X, et al. Glial TNFalpha in the spinal cord regulates neuropathic pain induced by HIV gp120 application in rats. *Molecular pain* 2011; **7**: 40

2 Chaplan SR, Bach FW, Pogrel JW, Chung JM, Yaksh TL. Quantitative assessment of tactile allodynia in the rat paw. *Journal of neuroscience methods* 1994; **53**: 55-63

3 Iida T, Yi H, Liu S, et al. Spinal CPEB-mtROS-CBP signaling pathway contributes to perineural HIV gp120 with ddC-related neuropathic pain in rats. *Experimental neurology* 2016; **281**: 17-27

4 Yi H, Liu S, Kashiwagi Y, et al. Phosphorylated CCAAT/enhancer binding protein beta contributes to rat HIV-related neuropathic pain, in vitro and in vivo studies. *The Journal of neuroscience : the official journal of the Society for Neuroscience* 2018; **38**: 555-74

5 Bava F-A, Eliscovich C, Ferreira PG, et al. CPEB1 coordinates alternative 3′ -UTR formation with translational regulation. *Nature* 2013; **495**: 121

6 Zheng X, Zheng W, Liu S, et al. Crosstalk between JNK and NF-kappaB in the KDO2-mediated production of TNFalpha in HAPI cells. *Cell Mol Neurobiol* 2012; **32**: 1375-83

7 Hao S, Liu S, Zheng X, et al. The role of TNFalpha in the periaqueductal gray during naloxone-precipitated morphine withdrawal in rats. *Neuropsychopharmacology : official publication of the American College of Neuropsychopharmacology* 2011; **36**: 664-76

8 Kim HY, Lee KY, Lu Y, et al. Mitochondrial Ca(2+) uptake is essential for synaptic plasticity in pain. *The Journal of neuroscience : the official journal of the Society for Neuroscience* 2011; **31**: 12982-91

9 Tymianski M, Bernstein GM, Abdel-Hamid KM, et al. A novel use for a carbodiimide compound for the fixation of fluorescent and non-fluorescent calcium indicators in situ following physiological experiments. *Cell Calcium* 1997; **21**: 175-83